

BB



SCAN-9506061

TRI-PP-95-10
March 1995 **${}^6\text{Li}(\pi^+, pp){}^4\text{He}_{g.s.}$ Reaction at 100 and 165 MeV Incident Pion Energies**Z. Papandreou*, G.M. Huber, G.J. Lolos, J.C. Cormier, E.L. Mathie, S.I.H. Naqvi
*Department of Physics, University of Regina, Regina, SK S4S 0A2 Canada*D.F. Ottewell, R. Tacik†, P.L. Walden
*TRIUMF, Vancouver, BC V6T 2A3 Canada*G. Jones, R.P. Trelle‡
*Department of Physics, University of British Columbia, Vancouver, BC V6T 2A6
Canada*X. Aslanoglou§
*Department of Physics and Astronomy, Ohio University, Athens, OH 45701-2979*D.L. Humphrey
*Department of Physics and Astronomy, Western Kentucky University, Bowling
Green, KY 42101***Abstract**

Differential and total cross sections for π^+ absorption on ${}^6\text{Li}$ leading to the $pp+{}^4\text{He}_{g.s.}$ final state are presented at incident pion energies of 100 and 165 MeV. The narrow width of the pp angular correlation is observed and reported for the first time.

(Submitted to Physical Review C)

PACS number(s): 25.80.Ls, 25.80.Hp

*Present Address: Department of Physics, The George Washington University, Washington, DC 20052

†Mailing Address: Department of Physics, University of Regina, Regina, SK, Canada, S4S 0A2

‡Present Address: Chemische Werke Bayer, Leverkusen, Germany

§Present Address: Department of Physics, University of Ioannina, Ioannina, Greece

Pion absorption has received considerable attention in the last decade due to its importance in the areas of pion-nucleus and heavy ion collisions. At incident pion energies below 1 GeV, the absorptive channel accounts for a significant portion of the total pion-nucleus cross section, and is thus of fundamental importance in understanding such interactions [1]. In addition, in heavy ion collisions where pions are created, many emerging pions are absorbed since the resonant pion mean free path in nuclear matter is only approximately 0.5 fm. In fact, in every field of investigation where pions and nuclei are in the initial and/or final state, the absorption process affects the primary physics in the reaction of interest.

It is clear, then, why such an important channel of pion-nucleus interactions has attracted experimental and theoretical investigations. Of particular interest in pion absorption on light nuclei is the contribution of absorption on $T = 0$ nucleon pairs (quasi-deuteron absorption or QDA) and the role of more complex reactions such as absorption by three nucleons (3NA). These two channels are conceptually the easiest to investigate and understand both theoretically and experimentally, but it is not yet clear whether they alone account for the total absorption cross section, or whether other channels are involved as well. The earlier claims of a small QDA contribution to the total cross section [2] have since been revised upward when more sophisticated experiments [3,4] were performed and individual specific final states were observed after pion absorption. Such experiments have been valuable in bringing to light the different angular distributions of specific states, after such a prediction was made earlier [5] as a critique of the method used in Ref. [2].

Generally, published results on pion absorption have attempted to correct for losses due to Final State Interactions (FSI), either through Intranuclear Cascade or DWIA calculations. The accuracy of such corrections, all based on QDA plus NN interactions in the exit channel, is an open question. The emission of three protons can signify either pion absorption on a correlated three nucleon cluster, or a two-step process based on QDA plus some form of FSI of one of the primary protons with an uncorrelated nucleon in the nucleus. Such FSI corrections have been found to be very significant for pion absorption on ${}^{16}\text{O}$ [3]. On the other hand, experiments on lighter nuclei with finer detector granularity [6] have not identified a clear contribution to the data by FSI, and have excluded any measurable contribution of Initial State Interactions followed by proper QDA. Given the recent results from $(e, e'p)$ reactions that have claimed a longer mean free path of protons in nuclei than expected [7], the absence of clear FSI signatures in very light nuclei is not all that surprising.

${}^6\text{Li}$ is an attractive choice of target for pion absorption investigations because it is one of a few light nuclei that allow specific final states to be observed with medium resolution, large acceptance detectors. This nucleus has been investigated at an incident pion energy of 59.4 MeV [8], where approximately 60% of the total pion absorption cross section could be accounted for by the transition to the ground and first excited states. However, that experiment only measured one angle pair ($60^\circ, -102.7^\circ$), and relied on a Monte Carlo simulation for their conclusions. Earlier results at 70 MeV [9] also found that the QDA mechanism dominates the ground state and low lying ${}^4\text{He}$ excited state transitions. The "BGO Ball Collaboration" investigated ${}^6\text{Li}$ at 50, 100, 150 and 200 MeV, and extracted different charged particle multiplicities [10,11]. However, these data have limited angular information due to the coarse ($\Delta\theta = 40^\circ$) detector granularity. The ${}^6\text{Li}(\pi^+, pp)$ reaction was also investigated [12] at 165 MeV

at KEK, and the authors claim that the broad components observed in the angular distributions are due to the two-step processes extracted from Ref. [13]. That work had good angular resolution, but was unable to extract total cross sections.

In the present work, we have investigated the ${}^6\text{Li}(\pi^+, pp){}^4\text{He}_{g.s.}$ reaction at incident pion energies of 100 and 165 MeV, with good angular resolution and coverage, in order to extract differential and total cross sections for the ${}^4\text{He}$ ground state transition. The detectors used in the present experiment have been described in detail elsewhere [14], so they will be only briefly described here.

The detectors consist of two assemblies of plastic scintillator positioned on either side of the TRIUMF M11 channel pion beam. Each assembly is further divided into two independent subassemblies, each covering 11 degrees in the horizontal scattering plane, and $\pm 11^\circ$ in the vertical plane. Each subassembly has a $\Delta E - E$ arrangement for particle identification, and the maximum proton stopping power is 220 MeV. Two (x, y) multi wire proportional chambers (MWPCs), in front of each assembly, were used for background rejection via two-arm trajectory extrapolation to the target. Most of the background was due to scattered pions and direct muons associated with the pion beam, and did not originate in the target. The pion flux was monitored using muon counters and in-beam plastic scintillator counters capable of counting individual muons and pions in the beam halo and in the beam itself. The target was mounted on a target holder made of plastic scintillator, thus necessitating carbon target subtraction by measuring the ${}^{12}\text{C}$ contribution to the pp channel. However, the Q values for the (π^+, pp) reactions on ${}^6\text{Li}$ and ${}^{12}\text{C}$ differ by 23.7 MeV, so the ${}^4\text{He}_{g.s.}$ transition is unaffected by the presence of the carbon in the multiple target assembly.

We have compared the data with Monte Carlo calculations using the ENIGMA [15] and GEANT codes [16]. The analysis and Monte Carlo methods will be reported in detail in a forthcoming publication on the ${}^{12}\text{C}(\pi^+, pp)$ reaction [17]. Briefly, the analysis employed particle identification, trajectory reconstruction and detector reaction loss recovery techniques to reconstruct the original energy of the detected protons in the center of the ${}^6\text{Li}$ target. All kinematic variables discussed below have been calculated using the full trajectory reconstruction from the MWPCs, each of which has a resolution of $< 0.25^\circ$ in the horizontal plane, and $< 0.5^\circ$ in the vertical plane. However, the angular distributions are quoted for the middle of each subassembly, and thus carry an intrinsic width of $\pm 5.5^\circ$ horizontal, and $\pm 11^\circ$ vertical.

A representative $E - E$ correlation (Dalitz plot) for 165 MeV incident pion energy is shown in Fig. 1a, which is 4° from quasi free absorption (QFA) kinematics. These data have energy loss and reaction loss corrections to the flux applied. In the figure, strong energy correlations due to the ${}^4\text{He}$ ground and excited final states are clearly visible, showing the underlying QDA nature of the absorption process for this angle pair. Contrast this energy correlation to Fig. 1b, which displays data taken 37° from QFA kinematics. Both Dalitz plots are normalized to the same number of incident pions and target thickness, and plotted with the same vertical scale, thus establishing the relative strength of the strongly correlated QDA protons in Fig. 1a with the three body phase-space-like distribution of Fig. 1b. The energy region far from the 2NA absorption correlation in Fig. 1a is very similar to the same region in Fig. 1b, further emphasizing that the main strength in Fig. 1a is due to QDA, and that 3NA and multi-step processes are small components of the total in-plane reaction cross section. These figures also demonstrate the absence of contributions under the ground state

peak from ${}^4\text{He}^*$ or phase-space-like transitions. Excitation spectra for the same two detector configurations are shown in Figs. 2a and 2b. The clear separation of the ground and excited states of ${}^4\text{He}$ is evident.

Figure 3 shows sample angular distributions for the ${}^6\text{Li}(\pi^+, pp){}^4\text{He}_{g.s.}$ reaction at 100 and 165 MeV. The width of the pp correlation is approximately 16° FWHM at both 100 and 165 MeV incident pion energies; this includes the finite width of the subassemblies, however, so the correlation could, in fact, be narrower. The dotted line indicates a QDA simulation which does not reproduce the width of the ${}^4\text{He}_{g.s.}$ transition. This is due to the Monte Carlo assumed momentum distribution for the nucleons involved in the absorption process, which although fitted to ${}^4\text{He}$, ${}^{16}\text{O}(e, e'p)$ data, and scaled for ${}^6\text{Li}$ via the number of target nucleons, does not include nuclear structure details. The narrowness of the ground state transition was predicted in Ref. [8] to be $\approx 13^\circ$, but could not be measured due to their limited angular coverage.

To obtain the $d\sigma/d\Omega^*$ shown in Fig. 4, the double differential cross sections were fitted with a Legendre polynomial series up to $P_{14}(\cos\theta)$, and integrated. These in turn were also fitted with Legendre polynomials (shown in the figure) to provide the total cross sections listed in Table I. The results in this table have had all experimental corrections applied, including reaction losses, edge effects, geometrical acceptance (derived from the Monte Carlo simulations) and energy losses in the target. No corrections have been made for FSI due to the reasons given in the introduction.

Early work from CERN [18] found the ratio of cross sections for the ${}^6\text{Li}(\pi^+, pp){}^4\text{He}_{g.s.}$ to the $\pi^+d \rightarrow pp$ reactions to be 0.91 ± 0.1 for incident pion energies between 50 and 275 MeV. The ratios for the data presented here are listed in Table I and shown in Fig. 5. The results of Ref. [11] appear to be low in comparison to both this work and Ref. [10] by the same authors. In terms of both the absolute cross section and the relative ratio, our result at 165 MeV is slightly smaller than at 100 MeV, and the 150 MeV result from Ref. [10] lies between our two values. This decreasing cross section with energy is a surprising result, which can only be understood by looking more closely at the angular distribution information. The pn pair in the initial ${}^6\text{Li}$ state is $l = 0$ with respect to the spin-0 ${}^4\text{He}$ core, and since the ${}^4\text{He}_{g.s.}$ final state is selected, the $l = 0$ pp system is therefore favored. Due to momentum transfer considerations, such an angular momentum configuration is more probable at 100 MeV than at 165 MeV. As seen in Fig. 4, the reaction is S-wave at 100 MeV, while at 165 MeV the $l = 0$ and $l = 2$ components interfere destructively near 90° .

In summary, we have measured the ${}^6\text{Li}(\pi^+, pp){}^4\text{He}_{g.s.}$ transition at incident pion energies of 100 and 165 MeV. This is the first time that this reaction has been measured with both good angular granularity and coverage, enabling the angular distribution of the pp correlation to be extracted. The measured width of $\approx 16^\circ$ (FWHM) at both energies is in reasonable agreement with the prediction of reference [8] at 59.4 MeV. Total cross sections were obtained by a Legendre polynomial integration of the measured angular distributions. The reaction is found to be essentially $l = 0$ at 100 MeV, but contains both $l = 0$ and $l = 2$ components at 165 MeV. We believe that this causes the cross section at 165 MeV to be slightly smaller than at 100 MeV. It should be also mentioned that a similar energy dependence has been observed recently on ${}^3\text{He}$, but no explanation was given [19].

ACKNOWLEDGEMENTS

We would like to thank Dr. J.L. Visschers for his extensive aid with the Monte Carlo program. This project was supported in part by the Natural Sciences and Engineering Research Council of Canada (NSERC), and the Saskatchewan Department of Economic Development. The generous assistance of Dr. E.W. Vogt, Director of TRIUMF, is also gratefully acknowledged.

REFERENCES

- [1] D. Ashery, J.P. Schiffer, *Ann.Rev. Nucl. Part. Sci.* **36** (1986) 207.
- [2] A. Altman et al., *Phys. Rev. C* **34** (1986) 1757.
- [3] S.D. Hyman et al., *Phys. Rev. C* **41** (1990) R409.
S.D. Hyman et al., *Phys. Rev. C* **47** (1993) 1184.
- [4] D.J. Mack et al., *Phys. Rev. C* **45** (1992) 1767.
- [5] B.G. Ritchie, N.S. Chant, P.G. Roos., *Phys. Rev. C* **30** (1984) 969.
- [6] P. Weber et al., *Phys. Rev. C* **43** (1991) 1553.
- [7] D.F. Geesaman et al., *Phys. Rev. Lett.* **63** (1989) 734.
- [8] R.Rieder et al., *Phys. Rev. C* **33** (1986) 614.
- [9] E.D. Arthur et al., *Phys. Rev. C* **11** (1975) 332.
- [10] R.D.Ransome et al., *Phys. Rev. Lett.* **64** (1990) 372.
- [11] R.D.Ransome et al., *Phys. Rev. C* **42** (1990) 1500.
- [12] H. Yokota et al., *Phys. Rev. C* **40** (1989) 1069.
- [13] H. Yokota et al., *Phys. Rev. Lett.* **58** (1987) 191.
- [14] Z. Papandreou et al., *Nucl. Instrum. Methods* **B34** (1988) 454.
- [15] J.L. Visschers, *Int. Conf. on Monte Carlo Simul. in High Energy and Nucl. Phys.*, World Scientific Co., Singapore (1994) 350.
- [16] CERN Computer Newsletter **200** (1990) 13.
- [17] G.M. Huber et al., to be published.
- [18] T. Bressani et al., *Nucl. Phys.* **B9** (1969) 427.
- [19] T. Altholz et al., *Phys. Rev. Lett.* **73** (1994) 1336.

Total Cross Sections σ (mb)

T_π (MeV)	${}^6\text{Li}(\pi^+, pp){}^4\text{He}_{g.s.}$	$\pi^+d \rightarrow pp[1]$	Ratio (Li/d)
50 [11]	5	6.78 ± 0.10	0.74
59.4 [8]	6.7	7.69 ± 0.14	0.87
100	12.9 ± 1.4	9.79 ± 0.13	1.32 ± 0.14
100 [11]	6		0.61
150 [10]	12.6 ± 1.9	11.70 ± 0.80	1.08 ± 0.17
150 [11]	8		0.68
165	10.0 ± 1.1	11.30 ± 0.50	0.88 ± 0.11
200 [11]	4	7.60 ± 0.60	0.53

Table 1: Total cross sections for this work, and from other sources as noted. The quoted errors for this work include both statistical and relative systematic uncertainties. The absolute systematic error is 15%. The results from reference [11] are estimates obtained by assuming that 40% of the published $2p\alpha + 2p{}^4\text{He}^*$ cross section is due to the ground state transition.

FIGURE CAPTIONS

Fig.1. Dalitz plots for the ${}^6\text{Li}(\pi^+, pp)$ reaction at 165 MeV incident pion energy for angle pairs: a) $(54.5^\circ, -95.5^\circ)$, b) $(54.5^\circ, -135.5^\circ)$. The diagonal bands in a) correspond to pure two nucleon absorption leading to the $pp + {}^4\text{He}_{g.s.}$ and $pp + {}^4\text{He}^*$ final states, while the triangular region at lower summed energy in both a), b) correspond to more complex absorption processes. Both a), b) are plotted with the same vertical scale (box size). A uniform detection threshold of 45 MeV (as calculated in the center of the target) is applied, and carbon background has been subtracted.

Fig.2. Recoil excitation histograms for the same angle pairs as shown in Fig. 1. The ground state cross sections presented here correspond to those events with excitation energy between -12 and +12 MeV.

Fig.3. $d^2\sigma/d\Omega^2$ angular distributions for the ${}^6\text{Li}(\pi^+, pp){}^4\text{He}_{g.s.}$ reaction at 100 MeV [filled squares] and 165 MeV [open squares]. In both a), b) the angle of one assembly is held fixed, while the other is scanned on the opposite side of the beam. The dotted curve is a QDA simulation at 165 MeV, arbitrarily normalized to the data. The difference between the two 100 MeV points in b) at $\theta_{p_2} = -84^\circ$ is taken into account in the relative systematic errors shown in Fig. 4.

Fig.4. $d\sigma/d\Omega^*$ angular distributions in the $\pi^+d \rightarrow pp$ center of momentum frame for the $pp + {}^4\text{He}_{g.s.}$ final state at a) 100 MeV and b) 165 MeV. The smooth curve is a Legendre polynomial fit $P_0 + P_2(\text{Cos}\theta^*)$.

Fig.5. Ratio of cross sections for the ${}^6\text{Li}(\pi^+, pp){}^4\text{He}_{g.s.}$ to the $\pi^+d \rightarrow pp$ reactions for the data listed in Table I.

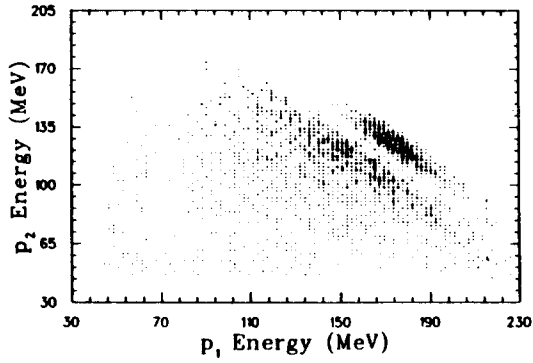


Fig. 1a

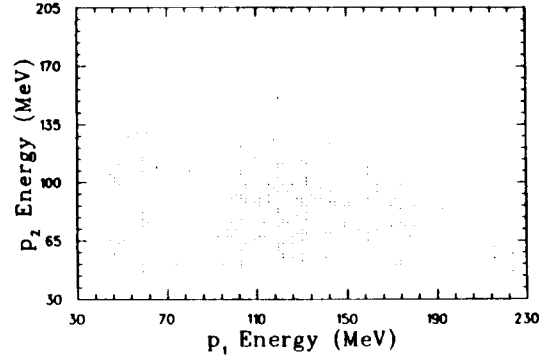


Fig. 1b

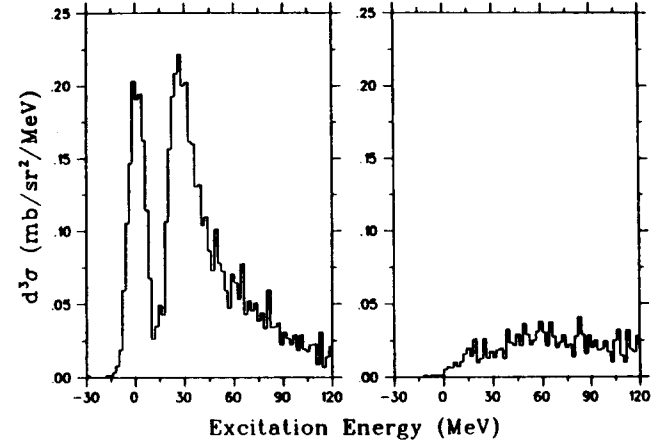


Fig. 2a

Fig. 2b

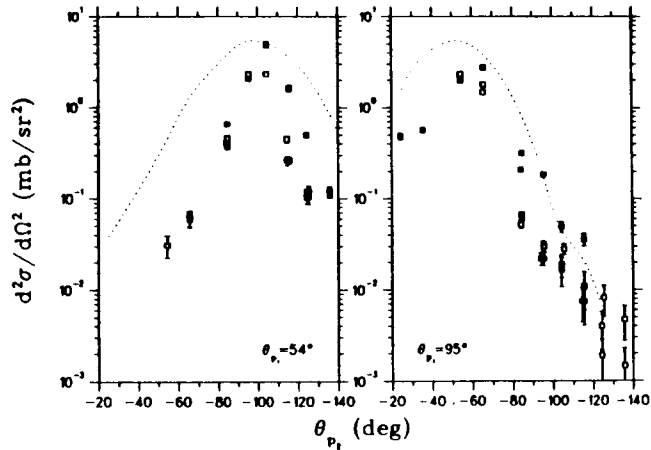


Fig. 3a

Fig. 3b

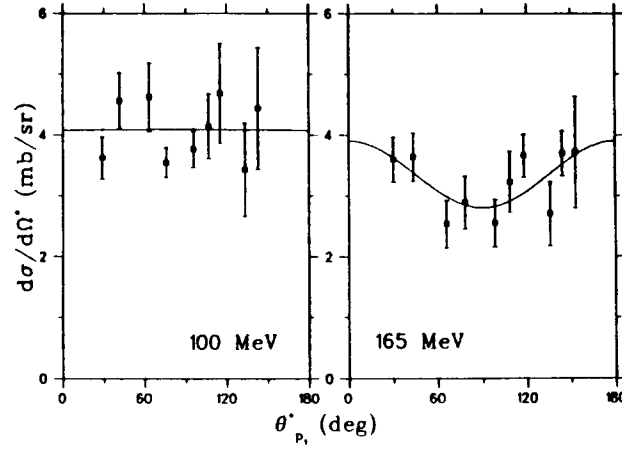


Fig. 4a

Fig. 4b

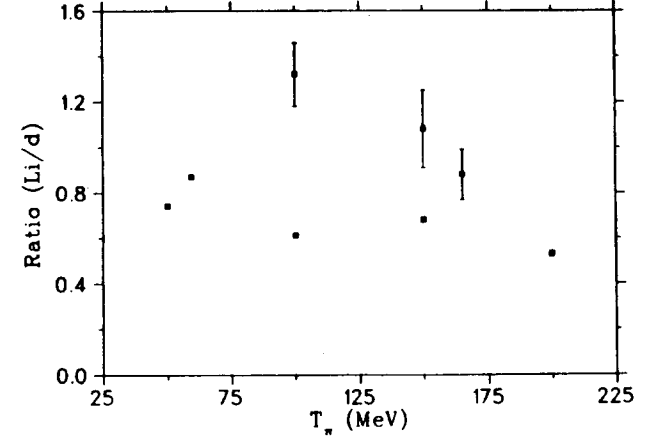


Fig. 5